Microfluid Nanofluid (2014) 17:519–526
DOI 10.1007/s10404-013-1328-0

RESEARCH PAPER

Deterministic fractionation of binary suspensions moving past a line of microposts

Raghavendra Devendra · German Drazer

Received: 13 August 2013 / Accepted: 27 December 2013 / Published online: 11 January 2014

Abstract We investigate the motion of suspended particles past a single line of equally spaced cylindrical posts that is slanted with respect to the driving force. We show that such a line of posts can fractionate particles according to their size, with small particles permeating through while the larger particles are deflected by the steric barrier created by the posts, even though the gaps between posts are larger than the particles. We perform characterization experiments driving monodisperse suspensions of particles of different size past the line of posts over the entire range of forcing orientations and present both the permeation probability through the individual gaps between the posts as well as the fraction of permeating particles through the one-dimensional array. In both cases, we observe a sharp transition from deflection to permeation mode that is a function of particle size, thus enabling separation. We then drive binary mixtures at selected orientations of the line of posts and demonstrate high separation purity and efficiency.

Keywords Separations · Microfluidics · Deterministic · Suspensions · Filtration · Fractionation

R. Devendra · G. Drazer
Department of Chemical and Biomolecular Engineering, Johns Hopkins University, Baltimore, MD 21218, USA
e-mail: raghu@jhu.edu

Present Address:
R. Devendra · G. Drazer (✉)
Department of Mechanical and Aerospace Engineering, Rutgers, The State University of New Jersey, Piscataway, NJ 08854, USA
e-mail: german.drazer@rutgers.edu

1 Introduction

An important unit operation in a variety of lab-on-a-chip systems is the separation of suspended mixtures of species. As a result, a number of microfluidic devices have been created either to miniaturize conventional separation techniques or to implement novel separation strategies (Stone et al. 2004; Pamme 2007; Li and Drazer 2007; Kulrattanarak et al. 2008; Lenshof and Laurell 2010). Different aspects of the separation process are emphasized depending on the application, but a common trend is the development of continuous separation processes, which can be readily integrated with downstream operations in a lab-on-a-chip platform (Yamada and Seki 2005; Huh et al. 2007; Bernate and Drazer 2011, 2012). A popular approach toward continuous separation processes is to create a selective barrier that is permeable to some species but deflects others. Various types of barriers have been explored including dielectrophoretic (Kralj et al. 2006; Alazzam et al. 2011), magnetophoretic (Pamme and Manz 2004; Zhu et al. 2012; Kirby et al. 2012), optical (Korda et al. 2002; MacDonald et al. 2003), and physical barriers (Belfort et al. 1994; De Jong et al. 2006; Gossett et al. 2010; Jaffrin 2012). A physical barrier is also at the core of the implementation of cross-flow filtration systems in microfluidic devices. In this method, suspended species are driven by a feed flow that is essentially tangent to a barrier membrane, and only permeable species move through the membrane driven by the pressure-driven cross-flow (VanDelinder and Groisman 2007; Ji et al. 2007; Aran et al. 2011). Let us point out that the main advantage of cross-flow filtration, compared to dead-end filtration in which all the flow passes through the membrane, is the reduction in clogging or fouling (VanDelinder and Groisman 2006; Ji et al. 2007). Note, however, that in all cases, it is the size of

the pores that separates between permeating (smaller) and deflected (larger) particles.

Deterministic lateral displacement (DLD) is another particularly promising, two-dimensional (2D) continuous separation method to fractionate a mixture of suspended species (Heller and Bruus 2008; Huang et al. 2004). In this technique, components of different size migrate in different directions as they are driven through a periodic array of cylindrical posts. DLD has been successfully implemented for the fractionation of diverse samples (Holm et al. 2011; Loutherback et al. 2010; Green et al. 2009; Long et al. 2008; Davis et al. 2006; Inglis et al. 2006). In our previous work, we investigated the mechanisms leading to separation in DLD and demonstrated an alternative operation mode, in which suspended species are driven through a 2D array of posts by a constant force, specifically gravity (g-DLD) (Devendra and Drazer 2012; Risbud and Drazer 2013; Bowman et al. 2012; Luo et al. 2011; Koplik and Drazer 2010; Balvin et al. 2009; Herrmann et al. 2009; Frechette and Drazer 2009). The motion of suspended particles in DLD devices exhibits directional locking, in which the migration angle remains constant and equal to a lattice direction over a finite range of forcing orientations (Frechette and Drazer 2009). In particular, for small enough angles between the external force and a line of posts corresponding to a column (or a row) in the square array, the particles move down a lane between two adjacent columns (or rows) without crossing them. Previous experiments also established that as the forcing angle increases (from zero), there is a critical transition angle, above which the particles are able to move across columns in the array (Devendra and Drazer 2012). This critical transition angle depends on particle size, thus allowing for separation. Moreover, the highest resolution of separation in a binary mixture was found to occur near the critical transition angle (Devendra and Drazer 2012). These results suggest that a single line or a one-dimensional (1D) array of cylindrical posts in lieu of the entire 2D array, could in principle, be used to fractionate a mixture of particles.

Here, motivated by our DLD results discussed above and the possibility of using steric barriers for separation, we investigate the motion of suspended particles driven past a slanted line of uniformly spaced cylindrical posts by a constant external force. We demonstrate that such a line of posts can, in fact, fractionate a mixture of suspended particles with high purity and efficiency. More specifically, we shall show that depending on the angle between the line of posts and the external force, large particles will be deflected sideways, whereas small particles will permeate through the line of posts. It is important to note that the gap between the posts is larger than the largest particles used here, unlike cross-filtration methods mentioned before. On the other hand, the deflection of particles of a given size is only possible when the *projected gap*, that is, the gap between posts projected in the direction of the driving force is smaller than the particles. The conceptual idea of the device is shown by the schematic in Fig. 1. This introduces a novel approach to separation based on a steric barrier (in this case, the single line of posts) that is fundamentally different from the traditional approach based on membranes or filters.

2 Experimental section

2.1 Device fabrication and experimental setup

The devices were fabricated using photolithography in a clean room. A negative photoresist (SU8-3025) was spun coated on top of a standard microscope glass slide, exposed to UV light, and developed to obtain a line of cylindrical posts on the glass slide. The thickness of the photoresist and, therefore, the height of the resulting posts, was approximately 40 μm. The profile of a fabricated line of

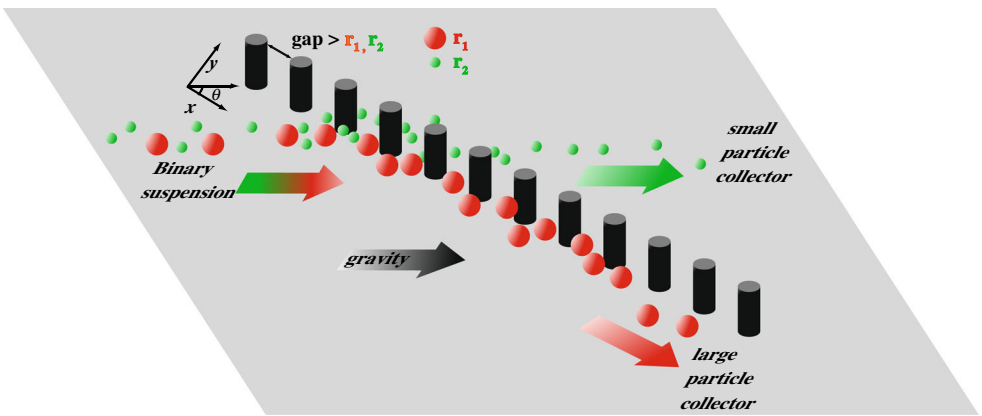

Fig. 1 Schematic representing the principle of operation of separation using single line of posts. r_1 and r_2 are representative radii of larger and smaller component in the binary mixture of particles, respectively

posts obtained with a 3D laser scanning microscope VK-X100/X200 (Keyence Corp., Japan) is shown in Fig. 2. The measured diameter of the posts is $2R = 19.5$ μm and the center-to-center separation is $\ell = 40$ μm. Several of these lines of posts were fabricated on a single glass slide. Individual lines of posts were separated by 1,000 μm from each other to avoid any effect on the particles moving past a given line from a neighboring line. The lines were used singularly in independent experiments. The diameter of the posts and the spacing between them were designed to be comparable to the diameter of the largest particles used in the experiments.

The lines of cylindrical posts were surrounded by double-sided adhesive tape (Grace Bio-Labs, Inc., OR) to create a containing well on the glass slide. We performed experiments using silica particles with a density of 2 g/cm^3 and average diameter of 4.32 μm (Bangs Laborarties, Inc., CA), 10, 15, and 20 μm (Corpuscular Inc., NY). The particles were suspended in 0.1 mM aqueous KOH solution (to prevent sticking). They were then introduced into the well and allowed to settle down at the bottom of the device. Without trapping any air inside, the well was sealed using a glass cover-slip (and double-sided adhesive tape) to eliminate the possibility of convective effects. The device containing the suspended particles was then mounted on a microscope, and the microscope was tilted at an angle, $\phi = 16°$, thus exploiting gravity to drive the particles down the slide and past the line of cylindrical posts. The average velocity of the particles in our experiments varied from 0.3 to 5 μm/s and dominates over other modes of transport such as diffusion. In fact, using the Stokes–Einstein equation for the bulk diffusivity of the particles and the distance between posts as the characteristic length, the corresponding Péclet

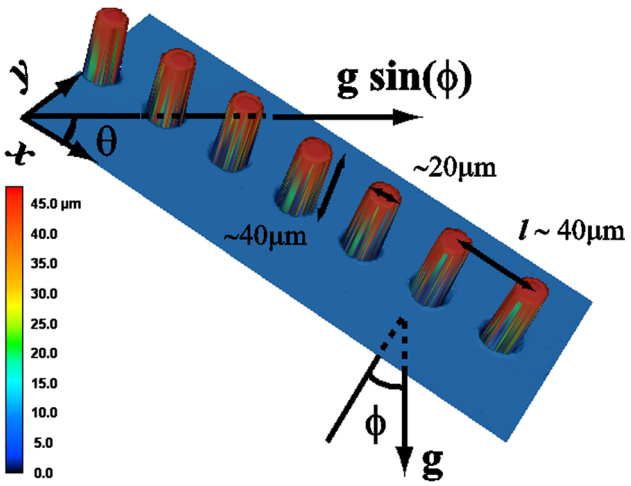

Fig. 2 Three-dimensional microscopic image of the device using a 3D laser scanning microscope. The color at *each point* represents the measured height. We indicate the microscope tilt angle ϕ, the forcing angle θ, the diameter of the posts $2R \approx 20$ μm, the spacing between the posts $\ell = 40$ μm, and the height of the posts ≈ 40 μm

numbers are $Pe > 100$, and Brownian motion is negligible. The Reynolds number based on these velocities is $Re < 10^{-3}$, and inertia effects can be ignored (Luo et al. 2011). More details on the experimental procedure can be found in Devendra and Drazer 2012.

2.2 Image acquisition and data analysis

Images were captured at a frame interval of 2s in bright field, using a Rolera Mgi+ EMCCD camera (Q-imaging, BC) and IPLab software (Biovision Tech, PA). We used manual tracking plugin (by Fabrice Cordelieres) in ImageJ (NIH, MD) to track the particles. The field of view consisted of 21 posts. The stream of particles was not focused from a single starting point, and as a result, the first interacting post for a given particle could be any one of the posts in the field of view. The forcing angle, θ, is defined as the angle between the direction of the driving force (gravity projected onto the plane of the device, i.e. *xy*-plane in Fig. 2) and the line of posts (*x*-axis in Fig. 2) and was measured by tracking particles in an (open) area free of posts. Experiments were performed independently at forcing angles with no particular increasing or decreasing order to avoid any cumulative error or correlation between the experiments. We only considered particles that travelled at least 100 μm in the driving direction to reduce fluctuations in the value of the measured forcing angle. The particles moving in the open area and those interacting with the posts were tracked separately. Approximately 20 particles were tracked in each experiment for a given forcing angle and a given particle size. In order to minimize the effect of polydispersity in the supplied particles, especially 10-, 15-, and 20-μm particles, we used calibration scales during tracking and considered only those particles within 10 % of the specified size. In order to capture the behavior in the dilute limit, the trajectories of particles that interact with another particle were discarded. On occasions, where a large particle blocked a spacing between the posts, the trajectories that interacted with such stuck particles were split into separate trajectories by cropping out the periods during which the interaction with the stuck particles took place. In rare instances, if a post was significantly different in size and shape from the design, the particles that interacted with that specific post were eliminated from the analysis.

3 Results and discussion

The proposed separation method is based on the hypothesis that we can use a single 1D array of cylindrical posts to fractionate a suspension of particles of different size into two streams. The main assumption is that, for a given particle size (and material), there is a critical forcing angle θ_c, which characterizes the motion of particles past the line

of posts. Specifically, particles would be displaced laterally by the line of posts for $\theta < \theta_c$ (*deflection mode*), but would pass through the line of posts for $\theta > \theta_c$ (*permeation mode*). The second assumption is that as observed in previous DLD experiments using 2D arrays of posts, the critical angle depends on particle size, thus leading to size-based separation (Devendra and Drazer 2012). In particular, a polydisperse suspension of particles moving past a line of posts oriented at an angle θ would result in two distinct streams of particles: a permeating stream, composed of particles for which $\theta_c < \theta$, and a deflecting stream moving along the line of posts, composed of all the particles for which $\theta_c > \theta$. Moreover, previous experiments in 2D arrays suggest that the critical forcing angle is an increasing function of particle size, and therefore, there would be a critical size $a = a_c$, where a is the particle radius, such that $\theta_c(a_c) = \theta$ and smaller particles ($a < a_c$) would simply permeate through the line of posts but larger particles ($a > a_c$) would be deflected.

3.1 Probability analysis

In order to investigate the postulated critical behavior, we analyze the motion and interaction of the particles with individual posts as independent stochastic events in a Bernoulli process. An event here is specific to a particle and a given gap between two consecutive posts. It is defined as a *success* if the particle passes through the gap and a *failure* if the particle does not pass through the gap but gets laterally displaced and continues toward the next gap downstream. Then, we define the probability of crossing, p, as the frequency ratio v_c/n, where v_c is the number of successes, and n is the total number of events. We also estimate the uncertainty in the determination of the probability of crossing with the standard deviation $\sigma_c = \sqrt{\frac{p(1-p)}{n}}$. We characterize the downstream output by defining a permeation fraction, $r_p = v_c/N$, where N is the total number of particles interacting with the line of posts. The uncertainty in the determination of the permeation fraction is estimated with the standard deviation $\sigma_p = \sqrt{\frac{p(1-p)}{N}}$. In terms of the experimental variables, θ_c is estimated as the average of the lower bound $\left(\theta_c^L\right)$ and upper bound $\left(\theta_c^U\right)$ values of the critical transition angle, defined by the largest forcing angle for which $p = 0$ and the smallest measured forcing angle for which $p = 1$, respectively.

3.2 Experimental results

In Fig. 3, we present the probability of crossing, p, as a function of the forcing angle, θ, for all particle sizes and the entire range of forcing directions. Each probability value is obtained from an independent experiment at the corresponding forcing angle. In all cases, we observe that the value of the probability is initially zero for a range of forcing directions and sharply transitions to $p = 1$ over a small range of forcing angles. This behavior is consistent with the directional locking observed in the 2D arrays (Devendra and Drazer 2012) and with the existence of a critical angle at which the motion of a given size of particles transitions from deflection to permeation, as discussed above. It is also clear in Fig. 3 that the critical angle is different for particles of different size, thus indicating the potential for using a single line of posts for separation. Both θ_c^L and θ_c^U increase with the size of the particles. The measured values are shown in Table 1, where we also estimate θ_c as the average between θ_c^L and θ_c^U. The estimated critical angle also shows the same trend as in 2D arrays (Devendra and Drazer 2012).

The actual separation, however, is better characterized by the fraction of particles that permeates through the line of posts, that is, the permeation fraction, r_p. In Fig. 4, we present r_p as a function of the forcing angle, θ, for all particle sizes. The transition from deflection to permeation is steeper, by definition of r_p, with the permeation angles at which $r_p = 1$, θ_p^U, typically reduced by $\approx 2°$ compared to θ_c^U. Note that by definition, $\theta_p^U \leq \theta_c^U$ and $\theta_p^L = \theta_c^L$. The measured values are shown in Table 1, where we also estimate θ_p as the average between θ_p^L and θ_p^U.

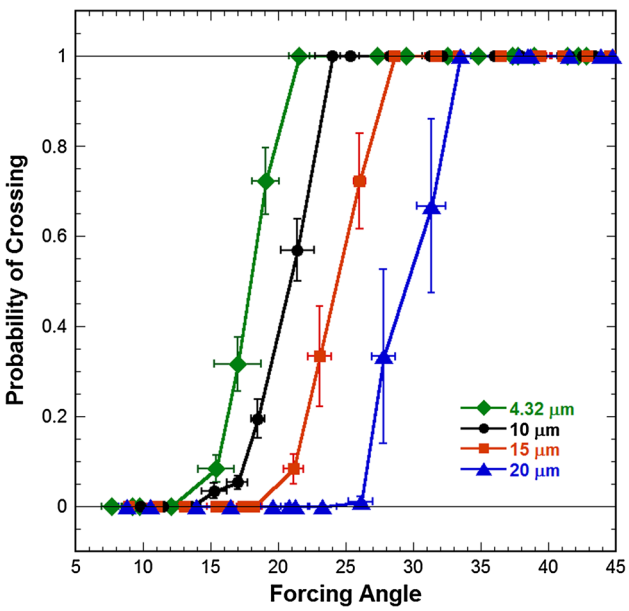

Fig. 3 Probability of crossing, p, for 4.32-, 10-, 15-, and 20-μm particles as a function of forcing angle

Table 1 Critical forcing angles for all particles in single species experiments

Particle diameter (μm)	θ_c^L	θ_c^U	θ_c	θ_p^L	θ_p^U	θ_p
4.32	$14° \pm 3°$	$20° \pm 2°$	$17° \pm 4°$	$14° \pm 3°$	$18° \pm 1°$	$16° \pm 4°$
10	$14° \pm 2°$	$23° \pm 3°$	$19° \pm 4°$	$14° \pm 2°$	$23° \pm 3$	$19° \pm 4°$
15	$20° \pm 1°$	$27° \pm 1°$	$23° \pm 2°$	$20° \pm 1°$	$25° \pm 1°$	$22° \pm 3°$
20	$25° \pm 2°$	$32° \pm 2°$	$29° \pm 4°$	$25° \pm 2°$	$30° \pm 2°$	$27° \pm 4°$

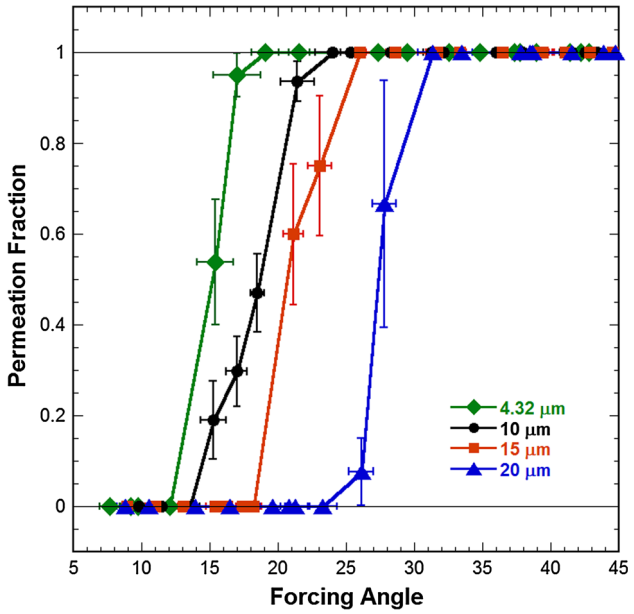

Fig. 4 Permeation fraction, r_p, for 4.32-, 10-, 15-, and 20-μm particles as a function of forcing angle

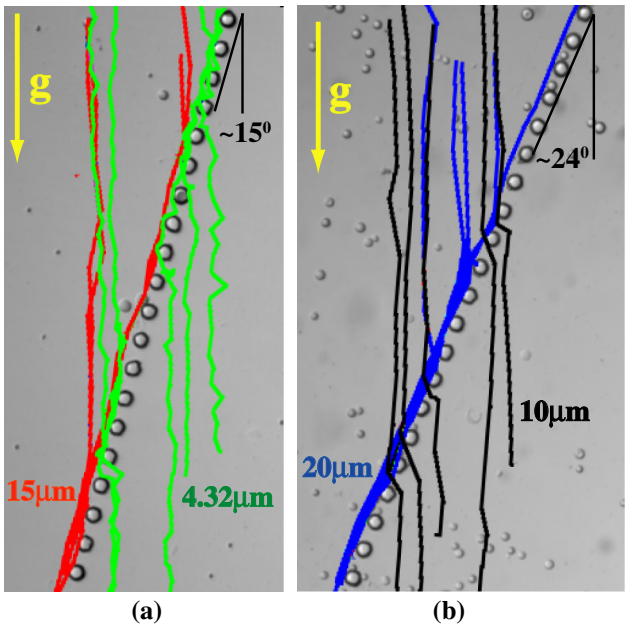

Fig. 5 Representative trajectories during the fractionation of two different binary mixtures. In both cases, we see permeation of the smaller particles in the mixture and deflection of the larger ones. **a** A mixture of 4.32- and 15-μm particles, $\theta = 15°$. **b** A mixture of 10- and 20-μm particles, $\theta = 24°$

3.3 Binary experiments and separability

Based on the results discussed above, obtained for different species separately, we selected specific forcing directions to investigate the separation of binary mixtures of 4.32- and 15-μm particles and of 10- and 20-μm particles. The purpose is to identify specific forcing directions where smaller particles permeate through the line of posts, while the larger particles deflect and to measure the separation efficiency and purity. In Fig. 5, we present particle trajectories from two representative examples of separation in binary mixtures.

In Fig. 5a, the forcing direction is $\theta \approx 15°$ and the 4.32-μm particles exhibit a finite permeation fraction ($0 < r_p < 1$), whereas the 15-μm particles are completely deflected along the direction of the line of posts ($r_p = 0$). In Fig. 5b, the forcing direction is $\theta \approx 24°$, and all the 10-μm particles permeate through the posts ($r_p = 1$), while all the 20-μm particles are completely deflected ($r_p = 0$). These figures graphically illustrate the probability analysis discussed above, as well as the proposed mechanism for separation.

In Fig. 6, we present the probability of crossing at the selected forcing directions, both in a binary mixture of 4.32- and 15-μm particles (Fig. 6a) and of 10- and 20-μm particles (Fig. 6c). We also present the permeation fraction, r_p, of the smaller particle and the deflection fraction, $r_d = 1 - r_p$, of the larger particle in both binary mixtures (Fig. 6b, d). High purity and efficiency of separation are achieved when both r_p and r_d are close to 100 % for smaller and larger particles, respectively. In the case of 10- and 20-μm particles, one of the force orientations ($\theta \approx 23°$) results in ideal separation. On the other hand, for the mixture of 4.32- and 15-μm particles, we approximate the optimum separation angle as the average between the estimated critical angles from the experiments. The data are summarized in Table 2.

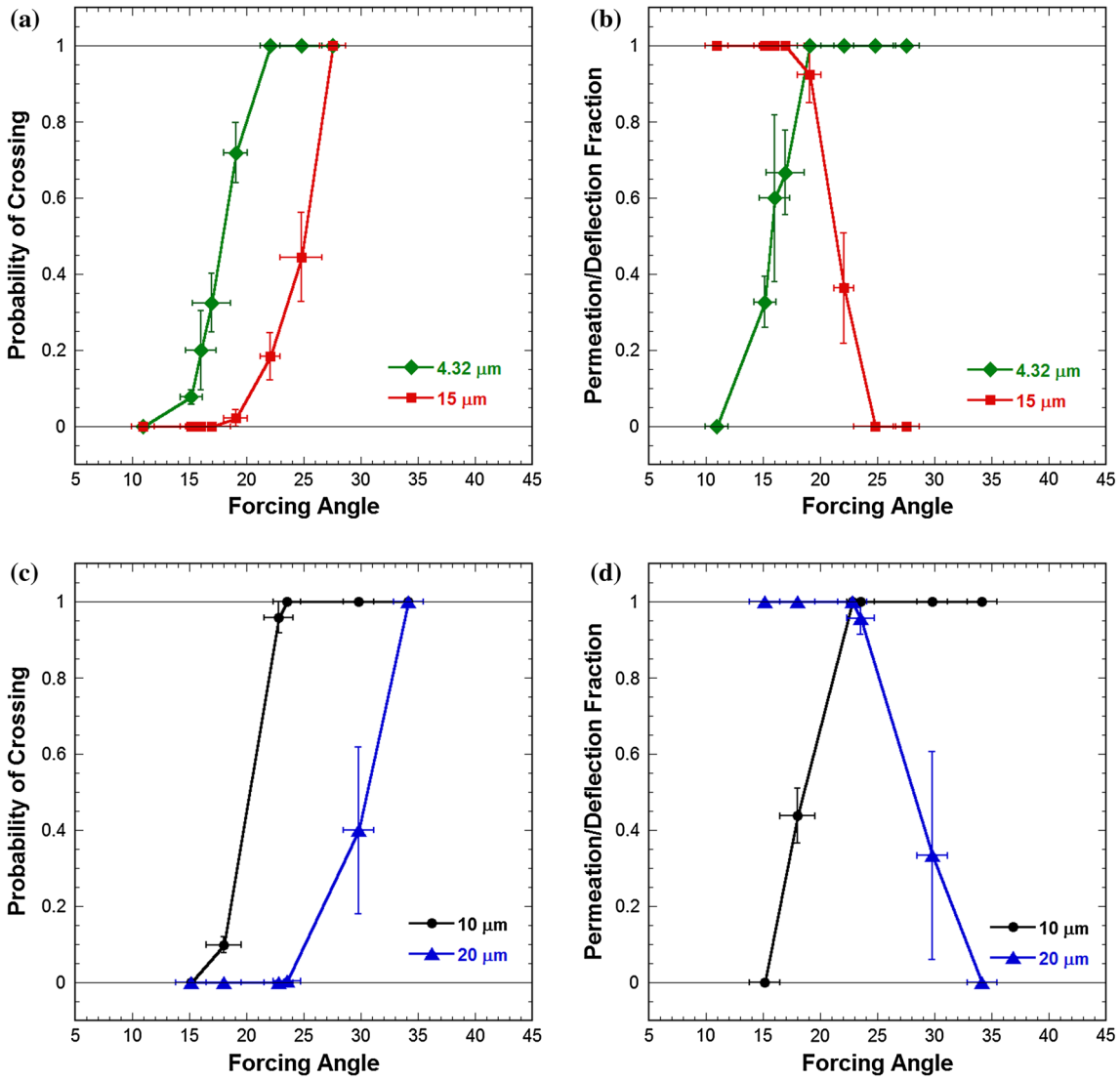

Fig. 6 Probability of crossing for a binary mixture of **a** 4.32- and 15-μm particles and of **c** 10- and 20-μm particles. Permeation fraction for 4.32- and 10-μm particles and deflection fraction for 15- and 20-μm particles in a binary mixture of **b** 4.32- and 15-μm particles and of **d** 10- and 20-μm particles

Table 2 Estimated optimum forcing angles for maximum separability in binary experiments

Particle diameter (μm)	θ_p	r_p (%)	r_d (%)
4.32	18° ± 3°	83 ± 6	17 ± 6
15	18° ± 3°	4 ± 4	96 ± 4
10	23° ± 1°	100	0
20	23° ± 1°	0	100

4 Conclusions

We presented a simple and novel method for continuously separating components in a binary mixture using a single line of cylindrical posts. We initially performed characterization experiments, by driving monodisperse suspensions through a line of posts over the entire range of forcing orientations and analyzed the results in terms of the probability of a particle to permeate through it. In each case, we observed a sharp increase in the permeation probability over a small range of forcing angles, indicating a transition from deflection to permeation mode as the forcing angle increases from zero. We also showed that the critical transition angle increases with particle size. We finally used these characterization experiments to fractionate binary mixtures at selected force orientations, showing excellent purity and efficiency of separation at angles close to the critical transition angle of the larger particles.

Let us finally note that, the probability of a particle to permeate through the line of posts depends on the number

of posts. It is expected that a longer line of posts increases the probability of crossing and thus, the permeation fraction. Hence, increasing the number of posts results in a shift toward lower values of the forcing angle at which all particles permeate, i.e., smaller θ_p^U. On the other hand, small variations in the size and shape of posts, as well as other effects such as Brownian motion of the suspended particles, could induce early transitions and lower the purity (or efficiency) of the separation. In this sense, a single line of posts is more sensitive to defects than a matrix of posts. Therefore, in a specific application, one should treat the number of posts as a variable used to optimize separation quality or resolution.

The separation approach proposed here has similarities with cross-flow fractionation, but it is important to note that in this case the size of the *pores* (openings between cylindrical posts) is larger than the size of the suspended particles. Therefore, the system is in principle less prone to clogging compared with traditional membrane-based filtration systems relying on the retention of particles larger that the membrane pores. Moreover, using post-post separations larger than the particles could also prevent clogging at larger volume fractions (and throughput) of the suspended mixture (VanDelinder and Groisman 2006; Bacchin et al. 2011; Henry et al. 2012) The study of clogging in this and similar microdevices is an important aspect that requires further attention (Wyss et al. 2006; Bacchin et al. 2011; Agbangla et al. 2012). Finally, let us mention that this method could be enhanced into multi-component separation by positioning consecutive lines of posts at increasing angles with respect to the force (or other arrangements).

Acknowledgments The authors acknowledge technical assistance in particle tracking by Roberto Passarro, Tsung-Chung Feng, and Siqi Du. This material is based upon work partially supported by the National Science Foundation under Grant CBET-0954840.

References

Agbangla GC, Climent É, Bacchin P (2012) Experimental investigation of pore clogging by microparticles: evidence for a critical flux density of particle yielding arches and deposits. Sep Purif Technol 101:42–48

Alazzam A, Stiharu I, Bhat R, Meguerditchian AN (2011) Interdigitated comb-like electrodes for continuous separation of malignant cells from blood using dielectrophoresis. Electrophoresis 32(11):1327–1336

Aran K, Fok A, Sasso LA, Kamdar N, Guan Y, Sun Q, Ündar A, Zahn JD (2011) Microfiltration platform for continuous blood plasma protein extraction from whole blood during cardiac surgery. Lab Chip 11(17):2858–2868

Bacchin P, Marty A, Duru P, Meireles M, Aimar P (2011) Colloidal surface interactions and membrane fouling: investigations at pore scale. Adv Colloid Interface Sci 164(1–2):2–11

Balvin M, Sohn E, Iracki T, Drazer G, Frechette J (2009) Directional locking and the role of irreversible interactions in deterministic hydrodynamics separations in microfluidic devices. Phys Rev Lett 103(7):078301

Belfort G, Davis RH, Zydney AL (1994) The behavior of suspensions and macromolecular solutions in crossflow microfiltration. J Membr Sci 96(1):1–58

Bernate JA, Drazer G (2011) Partition-induced vector chromatography in microfluidic devices. J Colloid Interface Sci 356(1):341–351

Bernate JA, Drazer G (2012) Stochastic and deterministic vector chromatography of suspended particles in one-dimensional periodic potentials. Phys Rev Lett 108(21):214501

Bowman T, Frechette J, Drazer G (2012) Force driven separation of drops by deterministic lateral displacement. Lab Chip 12(16):2903–2908

Davis JA, Inglis DW, Morton KJ, Lawrence DA, Huang LR, Chou SY, Sturm JC, Austin RH (2006) Deterministic hydrodynamics: taking blood apart. Proc Natl Acad Sci USA 103(40):14779–14784

De Jong J, Lammertink R, Wessling M (2006) Membranes and microfluidics: a review. Lab Chip 6(9):1125–1139

Devendra R, Drazer G (2012) Gravity driven deterministic lateral displacement for particle separation in microfluidic devices. Anal Chem 84(24):10621–10627

Frechette J, Drazer G (2009) Directional locking and deterministic separation in periodic arrays. J Fluid Mech 627:379–401

Gossett DR, Weaver WM, Mach AJ, Hur SC, Tse HTK, Lee W, Amini H, Di Carlo D (2010) Label-free cell separation and sorting in microfluidic systems. Anal Bioanal Chem 397(8):3249–3267

Green JV, Radisic M, Murthy SK (2009) Deterministic lateral displacement as a means to enrich large cells for tissue engineering. Anal Chem 81(21):9178–9182

Heller M, Bruus H (2008) A theoretical analysis of the resolution due to diffusion and size dispersion of particles in deterministic lateral displacement devices. J Micromech Microeng 18(7):075030

Henry C, Minier JP, Lefèvre G (2012) Towards a description of particulate fouling: from single particle deposition to clogging. Adv Colloid Interface Sci 185–186:34–76

Herrmann J, Karweit M, Drazer G (2009) Separation of suspended particles in microfluidic systems by directional locking in periodic fields. Phys Rev E 79:061404

Holm SH, Beech JP, Barrett MP, Tegenfeldt JO (2011) Separation of parasites from human blood using deterministic lateral displacement. Lab Chip 11(7):1326–1332

Huang LR, Cox EC, Austin RH, Sturm JC (2004) Continuous particle separation through deterministic lateral displacement. Science 304:987–990

Huh D, Bahng J, Ling Y, Wei H, Kripfgans O, Fowlkes J, Grotberg J, Takayama S (2007) Gravity-driven microfluidic particle sorting device with hydrodynamic separation amplification. Anal Chem 79(4):1369–1376

Inglis DW, Davis JA, Austin RH, Sturm JC (2006) Critical particle size for fractionation by deterministic lateral displacement. Lab Chip 6:655–658

Jaffrin MY (2012) Hydrodynamic techniques to enhance membrane filtration. Annu Rev Fluid Mech 44:77–96

Ji HM, Samper V, Chen Y, Heng CK, Lim TM, Yobas L (2007) Silicon-based microfilters for whole blood cell separation. Biomed Microdevices 10(2):251–257

Kirby D, Siegrist J, Kijanka G, Zavattoni L, Sheils O, O'Leary J, Burger R, Ducrée J (2012) Centrifugo-magnetophoretic particle separation. Microfluid Nanofluid 13(6):899–908

Koplik J, Drazer G (2010) Nanoscale simulations of directional locking. Phys Fluids 22:052005

Korda PT, Taylor MB, Grier DG (2002) Kinetically locked-in colloidal transport in an array of optical tweezers. Phys Rev Lett 89(12):128301

Kralj J, Lis M, Schmidt M, Jensen K (2006) Continuous dielectrophoretic size-based particle sorting. Anal Chem 78(14):5019–5025

Kulrattanarak T, van der Sman R, Schroën C, Boom R (2008) Classification and evaluation of microfluidic devices for continuous suspension fractionation. Adv Colloid Interface Sci 142(1):53–66

Lenshof A, Laurell T (2010) Continuous separation of cells and particles in microfluidic systems. Chem Soc Rev 39(3):1203–1217

Li Z, Drazer G (2007) Separation of suspended particles by arrays of obstacles in microfluidic devices. Phys Rev Lett 98(5):050602

Long BR, Heller M, Beech JP, Linke H, Bruus H, Tegenfeldt JO (2008) Multidirectional sorting modes in deterministic lateral displacement devices. Phys Rev E 78(4):046304

Loutherback K, Chou KS, Newman J, Puchalla J, Austin RH, Sturm JC (2010) Improved performance of deterministic lateral displacement arrays with triangular posts. Microfluid Nanofluid 9(6):1143–1149

Luo M, Sweeney F, Risbud SR, Drazer G, Frechette J (2011) Irreversibility and pinching in deterministic particle separation. Appl Phys Lett 99:064102

MacDonald M, Spalding G, Dholakia K (2003) Microfluidic sorting in an optical lattice. Nature 426(6965):421–424

Pamme N (2007) Continuous flow separations in microfluidic devices. Lab Chip 7(12):1644–1659

Pamme N, Manz A (2004) On-chip free-flow magnetophoresis: continuous flow separation of magnetic particles and agglomerates. Anal Chem 76(24):7250–7256

Risbud SR, Drazer G (2013) Trajectory and distribution of suspended non-brownian particles moving past a fixed spherical or cylindrical obstacle. J Fluid Mech 714:213–237

Stone HA, Stroock AD, Ajdari A (2004) Engineering flows in small devices: microfluidics toward a lab-on-a-chip. Annu Rev Fluid Mech 36:381–411

VanDelinder V, Groisman A (2006) Separation of plasma from whole human blood in a continuous cross-flow in a molded microfluidic device. Anal Chem 78(11):3765–3771

VanDelinder V, Groisman A (2007) Perfusion in microfluidic cross-flow: separation of white blood cells from whole blood and exchange of medium in a continuous flow. Anal Chem 79(5):2023–2030

Wyss HM, Blair DL, Morris JF, Stone HA, Weitz DA (2006) Mechanism for clogging of microchannels. Phys Rev E 74(6):061402

Yamada M, Seki M (2005) Hydrodynamic filtration for on-chip particle concentration and classification utilizing microfluidics. Lab Chip 5(11):1233–1239

Zhu T, Cheng R, Lee SA, Rajaraman E, Eiteman MA, Querec TD, Unger ER, Mao L (2012) Continuous-flow ferrohydrodynamic sorting of particles and cells in microfluidic devices. Microfluid Nanofluid 13(4):645–654